中國機械工程學刊第四十卷第三期第 239~247 頁(民國一百零八年)
Journal of the Chinese Society of Mechanical Engineers, Vol.40, No.3, pp 239~247 (2019)

The Evaluation of a Large-scale Optimization Model for Defect-free RSSR-SS Motion Generation

Wen-Tzong Lee*and Kevin Russell**

Keywords: RSSR-SS Linkage, Motion Generation, Constrained Nonlinear Optimization, Matlab

ABSTRACT

The Revolute-Spherical-Spherical-Revolute-Spherical-Spherical joint or RSSR-SS linkage is one of the most basic spatial multi-loop linkages in terms of its construction and its kinematics. In the authors' original work, a small-scale optimization model was presented and demonstrated for defect-free RSSR-SS linkage motion generation. By small-scale, we mean that the optimization model does not incorporate a general RSSR-SS kinematic displacement model and therefore, no function to explicitly minimize precision position error. In this work, a general RSSR-SS displacement model is fully incorporated in an optimization model to produce, for the first time, a large-scale optimization model with explicit precision position error minimization. This optimization model also includes constraints to eliminate order, branch and circuit defects-defects that are often encountered in classical dyad-based motion generation. With this large-scale optimization model, the dimensions of defect-free RSSR-SS linkages required to approximate precision positions with minimum error are calculated. Therefore, the novelty of this work is the first-time development of an RSSR-SS motion generation model with a minimum error function that simultaneously considers order, branch and circuit defect elimination. In addition to presenting and demonstrating the large-scale optimization model, this work also conveys both the benefits and drawbacks realized when implementing the RSSR-SS optimization model on a personal computer using the commercial mathematical analysis software package Matlab.

Paper Received November, 2017. Revised December, 2018. Accepted December, 2018. Author for Correspondence:Wen-Tzong Lee.

* *Department of Biomechatronics Engineering, National Pintung University of Science and Technology, Pingtung, 91201, Taiwan.*

** *Department of Mechanical and Industrial Engineering, New Jersey Institute of Technology, Newark, New Jersey 07102, USA*

INTRODUCTION

The RSSR-SS Linkage

The *Revolute-Spherical-Spherical-Revolute-Spherical-Spherical* joint or RSSR-SS linkage (Figure 1) is a particular type of *spatial multi-loop linkage*. Because this linkage is comprised of three link pairs or *dyads* (2 R-S dyads and 1 S-S dyad) it is more structurally sound in caparison to single-loop four-bar spatial linkages and therefore more capable of supporting loads. Because single loop spatial linkages are comprised of only two dyads, they cannot match the structural stability of multi-loop linkages.

The RSSR-SS linkage is one of the most basic spatial multi-loop linkages in terms of construction and kinematics. Regarding basic construction, the RSSR-SS linkage is comprised of only 6 rigid links interconnected by 2 revolute joints and 4 spherical joints. In addition, this linkage requires no specific construction schemes for assembly (unlike spherical linkages or Bennett's linkage for example). Regarding basic kinematics, fully-controlled coupler link motion (the coupler link is the link that includes $\mathbf{p}_1$ in Fig. 1) of the RSSR-SS linkage is achieved by controlling the rotation of a single revolute joint. The RSSR-SS linkage is a simple, low-cost alternative to the six degrees of freedom robotic *Stewart platform manipulator* (Dasgupta and Mruthyunjaya, 2000).

Developments in RSSR-SS Linkage Design and Analysis

Contributions in the areas of RSSR-SS linkage design and analysis include a computer-aided method to design order and branch defect-free RSSR-SS linkages to achieve four partially exact and partially approximate coupler positions (Sandor et al.,1986). A dyad-based optimization model was presented for the kinematic analysis and design of adjustable RSSR-SS linkages to approximate combinations of prescribed coupler positions, velocities and accelerations (Russell and Sodhi, 2003a). A dyad-based small-scale optimization model was presented for RSSR-SS motion generation (Shen et al., 2014). A combined analytical-numerical model was developed for the kinematic displacement analysis of RSSR-SS linkages (Russell and Sodhi, 2003b). Also, a fully analytical model was developed for the kinematic displacement and velocity analysis of RSSR-SS linkages (Shen et al., 2012).

While the noted works all address various important design or analysis aspects of the RSSR-SS linkage, they each have particular limitations that make the contribution of this work relevant. For example, the work of Sandor et. al. presents a method that requires computer-aided design software for implementation (Sandor et al.,1986). The works of Shen et al. and Russell and Sodhi do not include constraints to explicitly minimize precision position error or ensure the elimination of order, branch and circuit defects (Shen et al., 2014; Russell and Sodhi, 2003a). The works of Russell and Sodhi and Shen et al. were not developed to calculate the dimensions of RSSR-SS linkages. Rather, being kinematic analysis models, they are used to analyze RSSR-SS linkages of known dimensions (Russell and Sodhi, 2003b; Shen et al., 2012).

Scope of Work

The novelty of this work is the first-time development of an optimization model for RSSR-SS motion generation that simultaneously considers precision position error minimization and order, branch and circuit defect elimination. This work also conveys both the benefits and drawbacks realized when implementing the RSSR-SS optimization model on a personal computer using the commercial mathematical analysis software package *Matlab.*

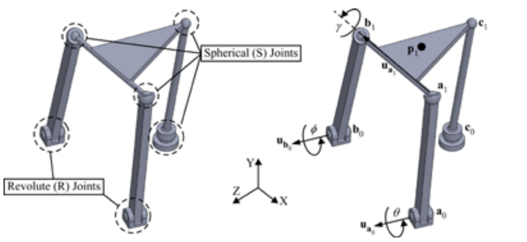

Figure 1 RSSR-SS linkage (left) with joint descriptions and (right) with displacement variables

GENERAL KINEMATIC DISPLACEMENT MODEL FOR THE RSSR-SS LINKAGE

A fully-analytical kinematic displacement model was presented for the RSSR-SS linkage (Shen et al., 2012). The displacements of moving pivots $\mathbf{a}_1$ and $\mathbf{b}_1$ result from the rotation of links $\mathbf{a}_0$ - $\mathbf{a}_1$ and $\mathbf{b}_0$ - $\mathbf{b}_1$ about their fixed-pivot joint axes by displacement angles θ and ϕ (Fig. 1). The displacements of $\mathbf{a}_1$ and $\mathbf{b}_1$ are given by

$$\mathbf{a} = \left[R_{\theta,\mathbf{u}_{\mathbf{a}_0}} \right] \left(\mathbf{a}_1 - \mathbf{a}_0 \right) + \mathbf{a}_0 \tag{1}$$

$$\mathbf{b} = \left[R_{\phi,\mathbf{u}_{\mathbf{b}_0}} \right] \left(\mathbf{b}_1 - \mathbf{b}_0 \right) + \mathbf{b}_0 \tag{2}$$

In these two equations, $\left[R_{\theta,\mathbf{u}_{\mathbf{a}_0}} \right]$ and $\left[R_{\phi,\mathbf{u}_{\mathbf{b}_0}} \right]$ are 3x3 spatial rotation matrices about the fixed pivot axis vectors $\mathbf{u}_{\mathbf{a}_0}$ and $\mathbf{u}_{\mathbf{b}_0}$ respectively (Fig. 1). The general form of the spatial rotation matrix (considering a rotation axis vector $\mathbf{u}$ and a displacement angle δ) is

$$\left[R_{\delta,\mathbf{u}} \right] = \begin{bmatrix} u_x^2 v(\delta) + \cos(\delta) & u_x u_y v(\delta) - u_z \sin(\delta) & u_x u_z v(\delta) + u_y \sin(\delta) \\ u_x u_y v(\delta) + u_z \sin(\delta) & u_y^2 v(\delta) + \cos(\delta) & u_y u_z v(\delta) - u_x \sin(\delta) \\ u_x u_z v(\delta) - u_y \sin(\delta) & u_y u_z v(\delta) - u_x \sin(\delta) & u_z^2 v(\delta) + \cos(\delta) \end{bmatrix} \tag{3}$$

where $v(\delta) = 1 - \cos(\delta)$.

The RSSR-SS kinematic displacement model is completed by including equations for the displacements of RSSR-SS moving pivot $\mathbf{c}_1$ and coupler point $\mathbf{p}_1$ (Fig. 1) (Shen et al., 2012). These equations are

$$\mathbf{c} = \left[R_{\gamma,\mathbf{u}_\mathbf{a}} \right] \left[R_{\omega,\mathbf{w}} \right] \left(\left[R_{\theta,\mathbf{u}_{\mathbf{a}_0}} \right] \left(\mathbf{c}_1 - \mathbf{a}_0 \right) + \mathbf{a}_0 - \mathbf{a} \right) + \mathbf{a} \tag{4}$$

$$\mathbf{p} = \left[R_{\gamma,\mathbf{u}_\mathbf{a}} \right] \left[R_{\omega,\mathbf{w}} \right] \left(\left[R_{\theta,\mathbf{u}_{\mathbf{a}_0}} \right] \left(\mathbf{p}_1 - \mathbf{a}_0 \right) + \mathbf{a}_0 - \mathbf{a} \right) + \mathbf{a} \tag{5}$$

It can be observed from the given spatial rotation matrices $\left[R_{\theta,\mathbf{u}_{\mathbf{a}_0}} \right]$, $\left[R_{\omega,\mathbf{w}} \right]$ and $\left[R_{\gamma,\mathbf{u}_\mathbf{a}} \right]$ that three distinct and simultaneous rotations comprise a single coupler link displacement in the RSSR-SS linkage (Shen et al., 2012). These rotations and their corresponding rotation axis vectors are illustrated in Figure 2. The coupler link rotates about the driving link fixed pivot axis vector $\mathbf{u}_{\mathbf{a}_0}$ by the driving link displacement angle θ. This rotation displaces the moving pivot $\mathbf{a}_1$ and the axis $\mathbf{u}_{\mathbf{a}_1}$ to $\mathbf{a}$ and $\mathbf{u}'_{\mathbf{a}_1}$ respectively (Fig 2a). The coupler link also rotates about a vector $\mathbf{w}$ by a displacement angle ω. Vector $\mathbf{w}$ is a unit vector orthogonal to the plane including vectors $\mathbf{u}_{\mathbf{a}_1}$ and $\mathbf{u}'_{\mathbf{a}_1}$. This rotation achieves the final moving pivot location $\mathbf{b}$ and displaces the axis $\mathbf{u}'_{\mathbf{a}_1}$ to $\mathbf{u}_{\mathbf{a}_1}$ (Fig 2b). Lastly, the coupler rotates about a vector $\mathbf{u}_\mathbf{a}$ by a displacement angle γ. This rotation achieves the final moving pivot location $\mathbf{c}$ and coupler point location $\mathbf{p}$ (Fig 2c).

Vector $\mathbf{u}_\mathbf{a}$ is produced by the displaced moving pivots $\mathbf{a}$ and $\mathbf{b}$ (therefore $\mathbf{u}_\mathbf{a} = (\mathbf{b}-\mathbf{a})/\|\mathbf{b}-\mathbf{a}\|$). Additionally, vector $\mathbf{w}$ (a coupler rotation axis vector formed by the cross product $\mathbf{u}'_{\mathbf{a}_1} \times \mathbf{u}_\mathbf{a}$) is defined as

$$\mathbf{w} = \frac{\mathbf{u}'_{\mathbf{a}_1} \times \mathbf{u}_\mathbf{a}}{\left|\mathbf{u}'_{\mathbf{a}_1} \times \mathbf{u}_\mathbf{a}\right|} \tag{6}$$

where

$$\mathbf{u}'_{\mathbf{a}_1} = \left[R_{\theta,\mathbf{u}_{\mathbf{a}_0}}\right]\mathbf{u}_{\mathbf{a}_1} \tag{7}$$

Vector $\mathbf{u}_{\mathbf{a}_1}$ is produced by the initial moving pivots $\mathbf{a}_1$ and $\mathbf{b}_1$ (therefore $\mathbf{u}_{\mathbf{a}_1} = (\mathbf{b}_1-\mathbf{a}_1)/\|\mathbf{b}_1-\mathbf{a}_1\|$). Being spatial rotation matrices, both $\left[R_{\omega,\mathbf{w}}\right]$ and $\left[R_{\gamma,\mathbf{u}_\mathbf{a}}\right]$ are identical in form to Equation (3).

The RSSR-SS variables $\mathbf{a}_0$, $\mathbf{a}_1$, $\mathbf{u}_{\mathbf{a}_0}$, $\mathbf{b}_0$, $\mathbf{b}_1$, $\mathbf{u}_{\mathbf{b}_0}$, $\mathbf{c}_0$, $\mathbf{c}_1$ and $\mathbf{p}_1$ are all 3x1 vectors containing *natural coordinates*-spatial Cartesian x, y and z-components.

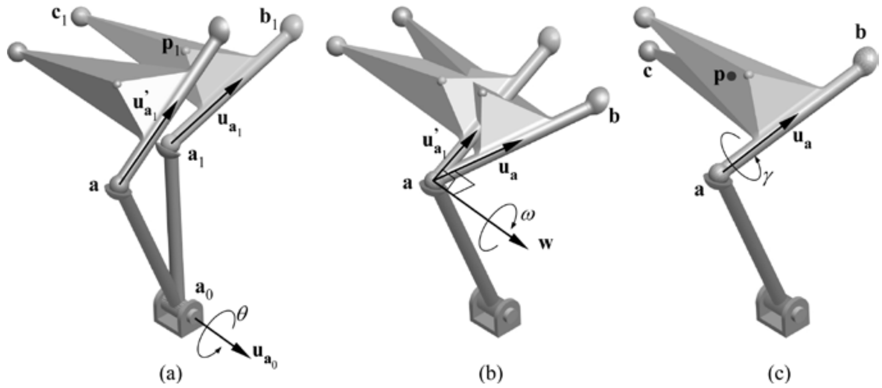

Figure 2 RSSR-SS (a) θ - $\mathbf{u}_{\mathbf{a}_0}$, (b) ω - $\mathbf{w}$ and (c) γ - $\mathbf{u}_\mathbf{a}$ coupler rotations

LARGE-SCALE OPTIMIZATION MODEL FOR DEFECT-FREE RSSR-SS MOTION GENERATION

What makes the optimization model in this work a large-scale model is that the entire general displacement model presented in the previous section is incorporated in it. This optimization model includes the objective function

$$f(\mathbf{X}) = \sum_{j=2}^{N}\left\{\left\|\mathbf{p}_j^* - \mathbf{p}_j\right\|^2 + \left\|\mathbf{q}_j^* - \mathbf{q}_j\right\|^2 + \left\|\mathbf{r}_j^* - \mathbf{r}_j\right\|^2\right\} \tag{8}$$

In Equation (8), $\mathbf{X} = \left(\mathbf{a}_0,\mathbf{a}_1,\mathbf{u}_{\mathbf{a}_0},\mathbf{b}_0,\mathbf{b}_1,\mathbf{u}_{\mathbf{b}_0},\mathbf{c}_0,\mathbf{c}_1,\theta_{1-2}\ldots\theta_{1-N},\phi_{1-2}\ldots\phi_{1-N},\gamma_{1-2}\ldots\gamma_{1-N}\right)$ which are all of the design variables for the RSSR-SS linkage (Fig. 1). Variables $\mathbf{p}_j^*$, $\mathbf{q}_j^*$ and $\mathbf{r}_j^*$ in Equation (8) represent the precision position coordinates and variables $\mathbf{p}_j$, $\mathbf{q}_j$ and $\mathbf{r}_j$ include the coupler position coordinates achieved by the calculated RSSR-SS linkage design. The equations for the displaced coupler points $\mathbf{q}_j$ and $\mathbf{r}_j$ are identical in form to Equation (5) where $\mathbf{p}$ and $\mathbf{p}_1$ are replaced with $\mathbf{q}$ and $\mathbf{q}_1$ respectively (or $\mathbf{r}$ and $\mathbf{r}_1$).

Equation (8) allows for the direct minimization of the error between the precision positions and the coupler positions achieved by the calculated RSSR-SS linkage design. An objective function having this capability is ideal since the linkage design should approximate the precision positions as closely as possible. As noted earlier, the authors' prior RSSR-SS optimization models do not incorporate the general RSSR-SS kinematic displacement model and therefore include no function to explicitly minimize precision position error (Shen et al., 2014; Russell and Sodhi, 2003a).

Along with the objective function, the optimization model includes three kinds of equality constraints. Equations (9) and (10) are unit vector constraints for joint axis vectors $\mathbf{u}_{\mathbf{a}_0}$ and $\mathbf{u}_{\mathbf{b}_0}$ (Fig. 1).

$$\left(\mathbf{u}_{\mathbf{a}_0}\right)^{\mathrm{T}}\left(\mathbf{u}_{\mathbf{a}_0}\right) - 1 = 0 \tag{9}$$

$$\left(\mathbf{u}_{\mathbf{b}_0}\right)^{\mathrm{T}}\left(\mathbf{u}_{\mathbf{b}_0}\right) - 1 = 0 \tag{10}$$

Equations (11) and (12) are orthogonality constraints to ensure that links $\mathbf{a}_1$ - $\mathbf{a}_0$ and $\mathbf{b}_1$ - $\mathbf{b}_0$ are orthogonal to joint axis vectors $\mathbf{u}_{\mathbf{a}_0}$ and

$\mathbf{u}_{\mathbf{b}_0}$ respectively throughout RSSR-SS motion (Fig. 1).

$$\left(\mathbf{u}_{\mathbf{a}_0}\right)^T\left(\mathbf{a}_j - \mathbf{a}_0\right) = 0, \quad j = 2 \ldots N \tag{11}$$

$$\left(\mathbf{u}_{\mathbf{b}_0}\right)^T\left(\mathbf{b}_j - \mathbf{b}_0\right) = 0, \quad j = 2 \ldots N \tag{12}$$

Equations (13) through (18) are constant length constraints for links $\mathbf{a}_1 - \mathbf{a}_0$, $\mathbf{b}_1 - \mathbf{b}_0$, $\mathbf{c}_1 - \mathbf{c}_0$ and coupler link distances $\mathbf{a}_1 - \mathbf{b}_1$, $\mathbf{a}_1 - \mathbf{c}_1$ and $\mathbf{b}_1 - \mathbf{c}_1$ respectively (Fig. 1). The displaced moving pivots $\mathbf{a}_j$, $\mathbf{b}_j$ and $\mathbf{c}_j$ are calculated using Equations (1), (2) and (4) from the RSSR-SS kinematic displacement model.

$$\left(\mathbf{a}_j - \mathbf{a}_0\right)^T\left(\mathbf{a}_j - \mathbf{a}_0\right) - \left(\mathbf{a}_1 - \mathbf{a}_0\right)^T\left(\mathbf{a}_1 - \mathbf{a}_0\right) = 0, \quad j = 2 \ldots N \tag{13}$$

$$\left(\mathbf{b}_j - \mathbf{b}_0\right)^T\left(\mathbf{b}_j - \mathbf{b}_0\right) - \left(\mathbf{b}_1 - \mathbf{b}_0\right)^T\left(\mathbf{b}_1 - \mathbf{b}_0\right) = 0, \quad j = 2 \ldots N \tag{14}$$

$$\left(\mathbf{a}_j - \mathbf{b}_j\right)^T\left(\mathbf{a}_j - \mathbf{b}_j\right) - \left(\mathbf{a}_1 - \mathbf{b}_1\right)^T\left(\mathbf{a}_1 - \mathbf{b}_1\right) = 0, \quad j = 2 \ldots N \tag{15}$$

$$\left(\mathbf{c}_j - \mathbf{c}_0\right)^T\left(\mathbf{c}_j - \mathbf{c}_0\right) - \left(\mathbf{c}_1 - \mathbf{c}_0\right)^T\left(\mathbf{c}_1 - \mathbf{c}_0\right) = 0, \quad j = 2 \ldots N \tag{16}$$

$$\left(\mathbf{a}_j - \mathbf{c}_j\right)^T\left(\mathbf{a}_j - \mathbf{c}_j\right) - \left(\mathbf{a}_1 - \mathbf{c}_1\right)^T\left(\mathbf{a}_1 - \mathbf{c}_1\right) = 0, \quad j = 2 \ldots N \tag{17}$$

$$\left(\mathbf{b}_j - \mathbf{c}_j\right)^T\left(\mathbf{b}_j - \mathbf{c}_j\right) - \left(\mathbf{b}_1 - \mathbf{c}_1\right)^T\left(\mathbf{b}_1 - \mathbf{c}_1\right) = 0, \quad j = 2 \ldots N \tag{18}$$

The RSSR-SS optimization model also includes three kinds of inequality constraints. Inequality (19) eliminates *branch defects* in the RSSR-SS linkage loop $\mathbf{a}_0 - \mathbf{a}_1 - \mathbf{b}_1 - \mathbf{b}_0$ because it ensures a constant cross product of link $\mathbf{b}_0 - \mathbf{b}$ and distance $\mathbf{b}_0 - \mathbf{a}$ (Balli and Chand, 2002; Mallik and Ghosh, 1994). A change in branch would result in a change in sign of the cross-products. Likewise, Inequality (20) eliminates branch defects in the RSSR-SS linkage loop $\mathbf{c}_0 - \mathbf{c}_1 - 0.5\left(\mathbf{a}_1 + \mathbf{b}_1\right) - 0.5\left(\mathbf{a}_0 + \mathbf{b}_0\right)$. Inequality (21) eliminates *order defects* (Balli and Chand, 2002; Mallik and Ghosh, 1994) because it ensures constant counter-clockwise crank rotation (or clockwise rotation if $\theta_j < \theta_{j-1}$ is used).

$$\left[\left(\mathbf{b}_j - \mathbf{b}_0\right) \times \left(\mathbf{a}_j - \mathbf{b}_0\right)\right] \cdot \left[\left(\mathbf{b}_1 - \mathbf{b}_0\right) \times \left(\mathbf{a}_1 - \mathbf{b}_0\right)\right] > 0, \quad j = 2 \ldots N \tag{19}$$

$$\left[\left(\mathbf{c}_j - \mathbf{c}_0\right) \times \left(\frac{\mathbf{a}_j + \mathbf{b}_j}{2} - \mathbf{c}_0\right)\right] \cdot \left[\left(\mathbf{c}_1 - \mathbf{c}_0\right) \times \left(\frac{\mathbf{a}_1 + \mathbf{b}_1}{2} - \mathbf{c}_0\right)\right] > 0, \quad j = 2 \ldots N \tag{20}$$

$$\begin{cases} \theta_j > \theta_{j-1} \\ \theta_N < 2\pi \end{cases} \quad j = 2 \ldots N \tag{21}$$

This combination of objective function and inequality constraints allows for the direct minimization of precision position error while simultaneously mitigating order and branch defects. And by including the entire closed-loop RSSR-SS kinematic displacement model in the optimization model, *circuit defects* are also mitigated (Balli and Chand, 2002; Mallik and Ghosh, 1994). In comparison, defect elimination cannot be ensured in RSSR-SS design methods where individual dyads are calculated and then assembled to produce the RSSR-SS linkage (Russell and Sodhi, 2003a; Sandor et al.,1986). For this work, this large-scale RSSR-SS optimization was implemented in the commercial mathematical analysis software *Matlab*.

OPTIMIZATION MODEL FILE SIZE COMPARISON IN MATLAB

The RSSR-SS optimization model presented in this work was codified in the commercial mathematical analysis software package Matlab and solved using the *interior-point algorithm* for constrained nonlinear optimization problems (Mathworks, 2018). While the RSSR-SS kinematic model and optimization model are given in matrix form, the full algebraic expansion of these models is required prior to solution calculation in Matlab.

The interior-point algorithm requires both the *gradient* and the *Hessian* of a constrained optimization model's objective function and nonlinear constraints (Mathworks, 2018). If the gradients and Hessians are not explicitly provided by the user, they will be estimated in Matlab. But as with any estimation, there is a possibility that it will poorly reflect reality. This possibility becomes more probable as the scale of the optimization model grows. Therefore, the best optimization model gradient and Hessian formulations would be algebraic formulations provided by the user (Mathworks, 2018). However, it is when algebraic gradients and Hessians are included in the RSSR-SS optimization model that implementation challenges become evident.

Table 1 includes the files sizes in Matlab of the fully-expanded RSSR-SS optimization model, its gradients and its Hessians formulated for 4 precision positions. The total file size of the fully-expanded optimization model (the $f\left(\mathbf{X}\right)$ column in Table 1) is 22.262 megabytes. An optimization model of this size is very manageable in Matlab on a 64-bit personal computer in terms of the memory required for solution calculation. The total size of the fully-expanded optimization model and gradients (the ∇f column in Table 1) is 7.3 gigabytes. An optimization model of this size remains manageable in Matlab on a 64-bit personal computer. However, the total size of the fully-expanded optimization model and gradients and Hessians (the $\mathbf{H}\left(f\right)$ column in Table 1) is 141 gigabytes-a size that makes the complete optimization impractical for use in

Matlab on even high-end personal computers.

Therefore, balancing the need to produce a robust but pc-manageable large-scale RSSR-SS optimization model resulted in the development of a 4-position RSSR-SS optimization model that includes gradients (but no Hessians) for a demonstration in this work.

Table 1 Equation, gradient and Hessian file sizes (in MB for $N=4$ coupler positions) in Matlab

Eq. No.	$f(\mathbf{X})$	∇f	$\mathbf{H}(f)$
8	7.692	2796	*62542
9	0.001	0.001	0.004
10	0.001	0.001	0.004
11	0.003	0.045	0.219
12	0.003	0.051	0.240
13	0.003	0.093	1.212
14	0.004	0.102	1.320
15	0.006	0.162	3.624
16	2.565	773.262	*17298
17	2.562	773.175	*17295
18	2.565	773.175	*17295
19	0.009	0.339	5.703
20	6.848	2170	*27363
sum	**22.262**	**7286**	***141805**

** estimated minimum file size*

EXAMPLE

Because the large-scale RSSR-SS optimization model has been formulated for only 4 precision positions (for the reasons explained in the previous section), an RSSR-SS linkage was designed to approximate the 4 positions in Figure 3. The (dimensionless) coordinates for these positions appear in Table 2. The objective in this example is to design a branch, order and circuit defect-free RSSR-SS linkage to approximate these positions.

Table 3 includes the initial values and calculated values for the RSSR-SS linkage dimensions. The initial values were not determined arbitrarily, but judiciously by graphically visualizing the precision positions in 3D space. By graphically visualizing the precision position in 3D space using *Computer Aided Design* (CAD) software, one can sketch spatial RSSR-SS linkages from which initial values are selected. Using this approach, the initial RSSR-SS dimension values for the optimization model are specified far more judiciously than they would by random guessing.

Table 4 includes the coupler positions achieved by the RSSR-SS linkage design (Figure 4). Table 5 includes the scalar differences between the precision positions and the coupler positions achieved by the RSSR-SS linkage design. Figure 5 includes plots of displacement angles ϕ and γ with respect to the driving link displacement angle θ. As shown by the continuity of the displacement angle plots in Fig. 5 and the coupler positions achieved by the RSSR-SS linkage design in Fig. 4 and Table 4, it is free of order, branch and circuit defects over the calculated driving link rotation range.

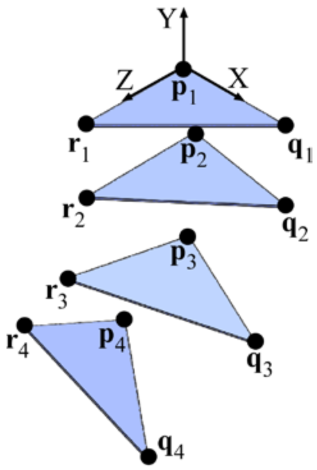

Figure 3 RSSR-SS precision positions

Table 2 Precision position coordinates

Pos. #	$\mathbf{p}^*$	$\mathbf{q}^*$	$\mathbf{r}^*$
1	0, 0, 0	5, 0, 0	0, 0, 5
2	1.416, −1.677, 0.881	6.374, −2.173, 1.290	0.952, −2.227, 5.828
3	2.388, −5.007, 2.165	6.918, −6.756, 3.356	1.088, −5.087, 6.992
4	0.196, −9.195, 3.184	3.081, −12.902, 4.898	−0.174, −7.342, 7.813

Table 3 Initial and calculated RSSR-SS linkage variable values

variable	initial values	calculated values
$\mathbf{a}_0$	−5, −10, 10	−1.814, −7.936, 7.795
$\mathbf{a}_1$	5, −5, 5	4.144, −6.723, 4.593
$\mathbf{u}_{\mathbf{a}_0}$	−0.5, −0.5, −0.5	−0.428, −0.216, −0.878
$\mathbf{b}_0$	−10, −5, 5	−9.308, −4.335, 4.491
$\mathbf{b}_1$	−5, 5, 5	−3.784, 0.323, 4.593
$\mathbf{u}_{\mathbf{b}_0}$	0.5, 0.5, 0.5	−0.136, 0.233, 0.963
$\mathbf{c}_0$	−5, −10, −5	−4.794, −8.798, −2.924
$\mathbf{c}_1$	−5, −5, −5	−0.628, −4.109, −0.569
$\theta_{1-2}, \theta_{1-3}, \theta_{1-4}$	40º, 80º,120º	21.501º, 57.992º, 118.746º
$\phi_{1-2}, \phi_{1-3}, \phi_{1-4}$	−20º,−30º,−40º	−16.303º, −35.327.º, −43.095º
$\gamma_{1-2}, \gamma_{1-3}, \gamma_{1-4}$	−10º,−15º,−20º	−10.762º, −21.344º, −12.970º
Number of Iterations: 253	Elapsed Time: 8867 seconds	

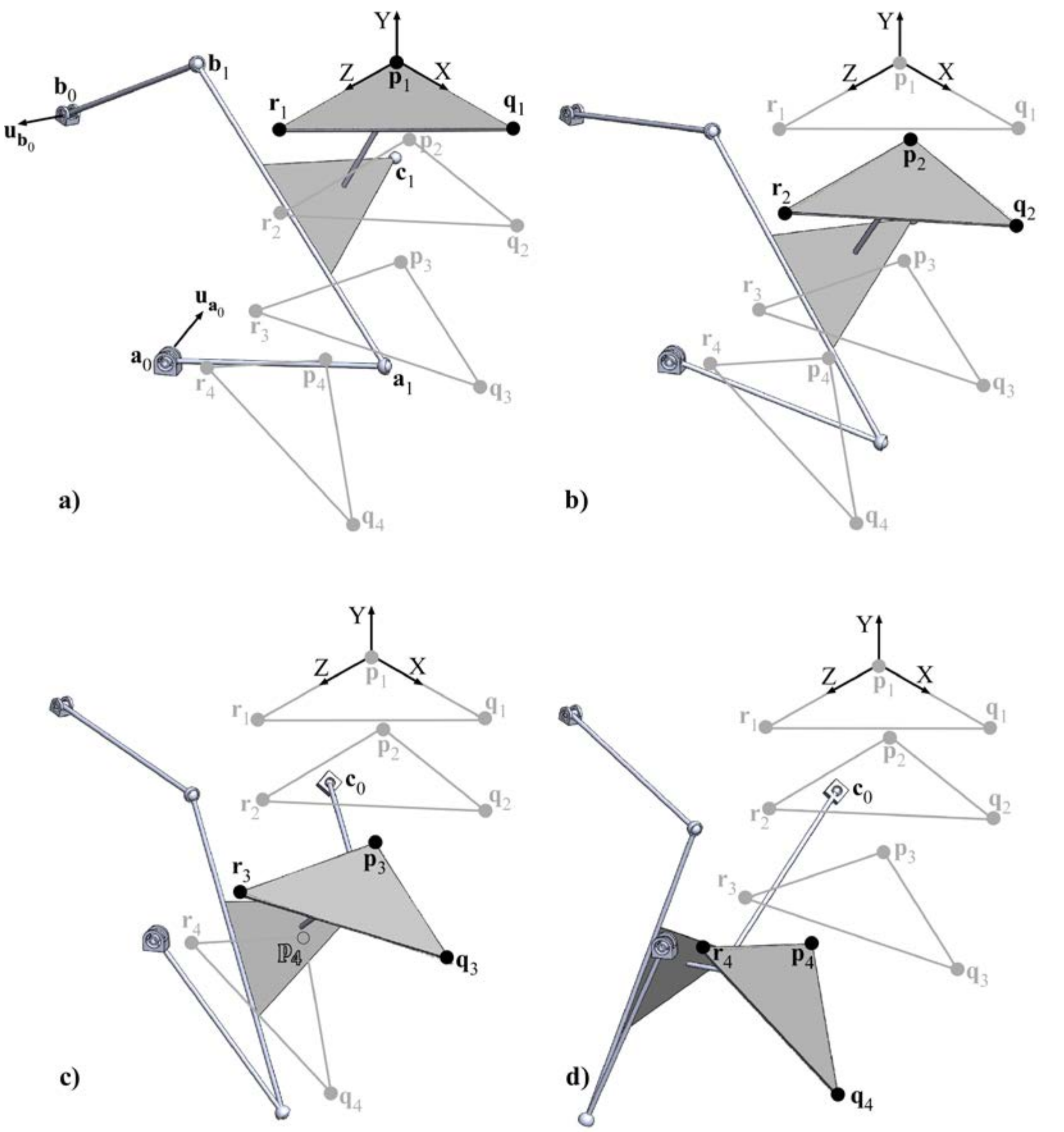

Figure 4 RSSR-SS linkage design at the achieved coupler positions 1 through 4 (Figs. 4a through 4d

respectively)

Table 4 Coupler position coordinates achieved by the RSSR-SS linkage design

Pos. #	$\mathbf{p}$	$\mathbf{q}$	$\mathbf{r}$
1	0, 0, 0	5, 0, 0	0, 0, 5
2	1.420, −1.681, 0.876	6.369, −2.256, 1.294	0.948, −2.136, 5.833
3	2.379, −4.995, 2.173	6.940, −6.685, 3.333	1.083, −5.181, 6.998
4	0.188, −9.234, −3.176	3.137, −12.859, 4.955	−0.215, −7.307, −7.772

Table 5 Scalar differences between he prescribed and achieved coupler positions

Pos. #	$\mathbf{p}^* - \mathbf{p}$	$\mathbf{q}^* - \mathbf{q}$	$\mathbf{r}^* - \mathbf{r}$
1	0, 0, 0	0, 0, 0	0, 0, 0
2	0.004, 0.004, 0.005	0.005, 0.083, 0.004	0.004, 0.091, 0.005
3	0.008, 0.012, 0.008	0.021, 0.071, 0.022	0.005, 0.095, 0.006
4	0.007, 0.039, 0.008	0.056, 0.043, 0.057	0.041, 0.035, 0.040

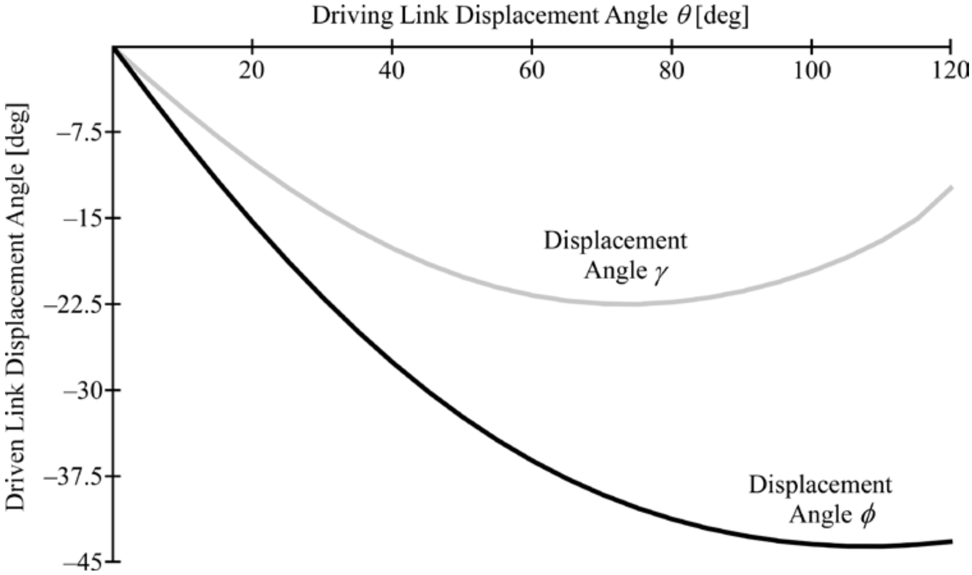

Figure 5 Driven link displacement angles (versus driving link rotation) for RSSR-SS linkage design

DISCUSSION

While the authors formulated an optimization model where all of the linkage dimensions are calculated, the user is free to exclude any dimension from among those to be calculated and prescribe them instead (e.g., fixed pivots $\mathbf{a}_0$, $\mathbf{b}_0$ and $\mathbf{c}_0$). Any excluded dimension will reduce the size of the gradients and Hessians of the optimization model.

The particular computing platform used to develop and run the 3-position RSSR-SS optimization model was a 64-bit Windows laptop with 16 gigabytes of memory and a 2.1 GHz processor. The amount of memory required to run a constrained optimization model is largely dependent on the number of variables included in the model. While there are only 33 specific types of variables in the optimization model used in Section 5, these variables appear over 1.5 million times in Equations (8) through (20) (for N=4) alone.

From Table 1, it can be observed that the largest equations, gradients and Hessians include either the displaced moving pivot $\mathbf{c}$ from Equation (4) or the displaced coupler point $\mathbf{p}$ from Equation (5). Both equations include the coupler rotation matrix $\left[R_{\omega,\mathbf{w}}\right]$ which includes the rotation axis vector $\mathbf{w}$ from Equation (6). The chief contributor to the sizes of Equations (8), (16) through (18) and Inequality (20) is the inclusion of the rotation axis vector $\mathbf{w}$. If an alternate analytical kinematic RSSR-SS displacement model could be formulated that does not require this coupler rotation, then it is possible that a much smaller and subsequently more manageable RSSR-SS optimization model could be produced.

Another possible option is to consider an alternate solution algorithm. *Evolutionary*

Algorithms are algorithms based on a natural selection process that mimics biological evolution. In the context of planar linkage design, the evolutionary algorithm method has been noted to offer the simplicity of implementation and fast convergence to the optimal solution with no need of a substantial knowledge of the solution space (Acharyya and Mandal, 2009; Cabrera et al., 2002). Perhaps the large-scale RSSR-SS optimization model would be a more manageable problem when solved using these algorithms.

CONCLUSION

For the first time, a large-scale optimization model for defect-free RSSR-SS linkage design to approximate precision positions was implemented in this work. With this optimization model, the dimensions of an order, branch and circuit defect-free RSSR-SS linkage with minimum precision position error were calculated. The primary drawbacks of the optimization model (in Matlab on a personal computer) are the large file sizes of the optimization model's algebraic gradients and Hessians.

REFERENCES

Acharyya, S. K. and Mandal, M., "Performance of EAs for Four-Bar Linkage Synthesis," *Mechanism and Machine Theory*, Vol. 44, No. 9, pp. 1784-1794 (2009).

Balli, S. S. and Chand, S., "Defects in Link Mechanisms and Solution Rectification," *Mechanism and Machine Theory*, Vol. 37, No. 9, pp. 851-876 (2002).

Cabrera, J. A., Simon, A. and Prado, M., "Optimal Synthesis of Mechanisms with Genetic Algorithms," *Mechanism and Machine Theory*, Vol. 37, No. 10, pp. 1165-1177 (2002).

Dasgupta, B. and Mruthyunjaya, T. S., "The Stewart Platform Manipulator: A Review," *Mechanism and Machine Theory*, Vol. 35, No. 1, pp. 15-40 (2000).

Mallik, A. K., Ghosh, A. and Dittrich, D., Kinematic Analysis and Synthesis of Mechanisms, CRC Press, Boca Raton (1994).

Mathworks: Constrained Nonlinear Optimization Algorithms. https://www.mathworks.com/help/optim/ug/constrained-nonlinear-optimization-algorithms.html (Accessed 11 March 2018).

Russell, K. and Sodhi, R. S., "Kinematic Synthesis of Adjustable RSSR-SS Mechanisms for Multi-Phase Finite and Multiply-Separated Positions," ASME Journal of Mechanical Design, Vol. 125, No. 4, pp. 847-853 (2003a).

Russell, K. and Sodhi, R. S., "On Displacement Analysis of the RSSR-SS Mechanism," Mechanics Based Design of Structures and Machines, Vol. 31, No. 2, pp. 281-296 (2003b).

Sandor, G. N., Xu, L. J. and Yang, S. P., "Computer-Aided Synthesis of Two-Closed-Loop RSSR-SS Spatial Motion Generator with Branching and Sequence Constraints" *Mechanism and Machine Theory*, Vol. 21, No. 4, pp. 345-350 (1986).

Shen, Q., Lee, W, and Russell, K., "A Small-scale Optimization Model for RSSR-SS Motion Generation with Branch and Order Defect Elimination in Matlab," Journal of Advanced Mechanical Design, Systems, and Manufacturing, Vol. 8, No. 3, pp. 00239 (2014).

Shen, Q., Russell, K. and Sodhi, R. S., "Analytical Displacement and Velocity Modeling of the RSSR-SS Linkage," Proceedings of the 11th International Conference on the Theory of Machines and Mechanisms, pp. 151-156 (2012).

APPENDIX

Notation

$\mathbf{a}_0$, $\mathbf{b}_0$, $\mathbf{c}_0$	RSSR-SS fixed pivots
$\mathbf{a}_1$, $\mathbf{b}_1$, $\mathbf{c}_1$	RSSR-SS moving pivots
$\mathbf{a}$, $\mathbf{b}$, $\mathbf{c}$	displaced RSSR-SS moving pivots
$\mathbf{u}_{\mathbf{a}_0}$, $\mathbf{u}_{\mathbf{b}_0}$	fixed pivot joint axes vectors
$\mathbf{u}_{\mathbf{a}_1}$, $\mathbf{w}$	coupler link rotation axis vectors
$\mathbf{u}_{\mathbf{a}}$	displaced coupler link rotation axis vector
θ	crank link angular displacement
λ	coupler link angular displacement
ϕ	angular displacement for follower link $\mathbf{b}_0$ - $\mathbf{b}_1$
$\mathbf{p}_1$, $\mathbf{p}$	coupler point and displaced coupler point respectively
$\left[R_{\theta,\mathbf{u}_{\mathbf{a}_0}}\right]$	rotation matrix about fixed pivot joint axis vector $\mathbf{u}_{\mathbf{a}_0}$
$\left[R_{\omega,\mathbf{w}}\right]$	rotation matrix about coupler rotation axis vector $\mathbf{w}$
$\left[R_{\gamma,\mathbf{u}_{\mathbf{a}}}\right]$	rotation matrix about displaced coupler rotation axis vector $\mathbf{u}_{\mathbf{a}}$
$\left[R_{\phi,\mathbf{u}_{\mathbf{b}_0}}\right]$	rotation matrix about fixed pivot joint axis vector $\mathbf{u}_{\mathbf{b}_0}$

大規模最佳化模型於無缺陷的 RSSR-SS 運動合成連桿的評估。

李文宗
國立屏東科技大學 生物機電工程學系
羅素‧凱文
紐澤西理工學院 機械與工業工程學系

摘 要

RSSR-SS 連桿是基本的空間多迴路連桿機構之一。在作者的前著作中，曾示範小規模的最佳化模型、無缺陷的運動合成連桿設計。對於小規模的最佳化模型，其最佳化模型並不包含一般的 RSSR-SS 運動位移方程式，並且不包括計算預定位置與合成位置之間的最小化誤差的函數。但是在本研究中， RSSR-SS 位移方程式將包含於最佳化模型中，這是首次設計一個具有位移誤差最小化的無缺陷 RSSR-SS 運動合成機構。利用此最佳化模型，計算出趨近預先規劃位置最小誤差所需的 RSSR-SS 合成機構。該最佳化模型亦包括降低順序，分支和迴路缺陷的約束方程式。除了示範最佳化模型之外，本研究亦討論使用數學分析軟件 Matlab 在個人電腦上實現 RSSR-SS 優化模型時的利弊。